Nanowire-Mediated Delivery Enables Functional Interrogation of Primary Immune Cells: Application to the Analysis of Chronic Lymphocytic Leukemia

NANO LETTERS

Letter

pubs.acs.org/NanoLett

Nanowire-Mediated Delivery Enables Functional Interrogation of Primary Immune Cells: Application to the Analysis of Chronic Lymphocytic Leukemia

Alex K. Shalek,[†,○] Jellert T. Gaublomme,[†,○] Lili Wang,[§,∥] Nir Yosef,[#] Nicolas Chevrier,[#] Mette S. Andersen,[‡] Jacob T. Robinson,[†] Nathalie Pochet,[#] Donna Neuberg,[⊥] Rona S. Gertner,[†] Ido Amit,[#] Jennifer R. Brown,[§] Nir Hacohen,[#] Aviv Regev,[#,▽] Catherine J. Wu,[§,∥] and Hongkun Park*[,†,‡]

[†]Department of Chemistry and Chemical Biology and [‡]Department of Physics, Harvard University, 12 Oxford Street, Cambridge, Massachusetts 02138, United States

[§]Department of Medicine, Harvard Medical School and [∥]Cancer Vaccine Center and [⊥]Department of Biostatistics and Computational Biology, Dana-Farber Cancer Institute, Boston, Massachusetts 02115, United States

[#]Broad Institute of MIT and Harvard, 7 Cambridge Center, Cambridge, Massachusetts 02142, United States

[▽]Howard Hughes Medical Institute, Department of Biology, Massachusetts Institute of Technology, Cambridge, Massachusetts 02140, United States

Supporting Information

ABSTRACT: A circuit level understanding of immune cells and hematological cancers has been severely impeded by a lack of techniques that enable intracellular perturbation without significantly altering cell viability and function. Here, we demonstrate that vertical silicon nanowires (NWs) enable gene-specific manipulation of diverse murine and human immune cells with negligible toxicity. To illustrate the power of the technique, we then apply NW-mediated gene silencing to investigate the role of the Wnt signaling pathway in chronic lymphocytic leukemia (CLL). Remarkably, CLL-B cells from different patients exhibit tremendous heterogeneity in their response to the knockdown of a single gene, *LEF1*. This functional heterogeneity defines three distinct patient groups not discernible by conventional CLL cytogenetic markers and provides a prognostic indicator for patients' time to first therapy. Analyses of gene expression signatures associated with these functional patient subgroups reveal unique insights into the underlying molecular basis for disease heterogeneity. Overall, our findings suggest a functional classification that can potentially guide the selection of patient-specific therapies in CLL and highlight the opportunities for nanotechnology to drive biological inquiry.

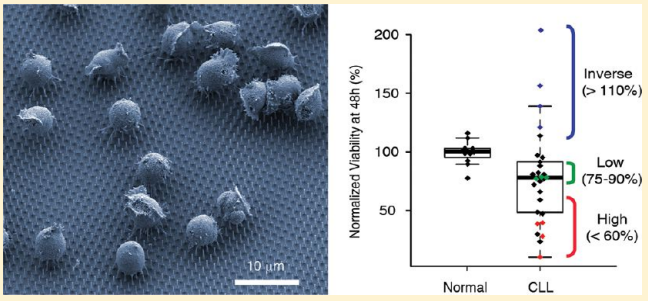

KEYWORDS: *Nanowires, delivery, immune cells, perturbation, chronic lymphocytic leukemia*

Achieving a circuit-level understanding of cellular function requires techniques to systematically perturb intracellular components and measure cellular responses. Since most perturbing agents (plasmid DNAs, siRNAs, peptides, and proteins) do not spontaneously cross the cell membrane with high efficiency, a host of methods has been developed to deliver various biological effectors into living cells.[1−4] Unfortunately, in primary immune cells[1−9] and especially in resting cells and lymphocytes,[6,7] these traditional approaches have proven ineffective. Specifically, common lipid and cationic delivery reagents[1,5,7,9,10] yield low transfection efficiencies and induce nonspecific inflammation in these cells[1−3,9] because the endocytic pathways upon which these methods rely are carefully gated via foreign element detectors (e.g., toll-like receptors[11]). Viral vectors fare poorly for similar reasons and also due to the presence of cytoplasmic viral nucleic acid sensors.[2,3,6,11] Electroporation/nucleofection, which enables delivery by temporarily breaking-down the cellular membrane through the application of an electric field,[4,7,8,12,13] achieves only mild success because, even with specialized protocols and buffers, immune cells undergo pervasive apoptosis after electroporation. This resistance to conventional transfection has been a major stumbling block in characterizing the molecular circuits responsible for primary immune cell function and highlights the urgent need to develop new approaches for efficiently perturbing these cells.

Vertical silicon nanowires (NWs) provide a powerful new delivery modality for administering biomolecular perturbants directly into the cell cytoplasm.[14] Previous studies have shown

Received: November 20, 2012
Published: November 28, 2012

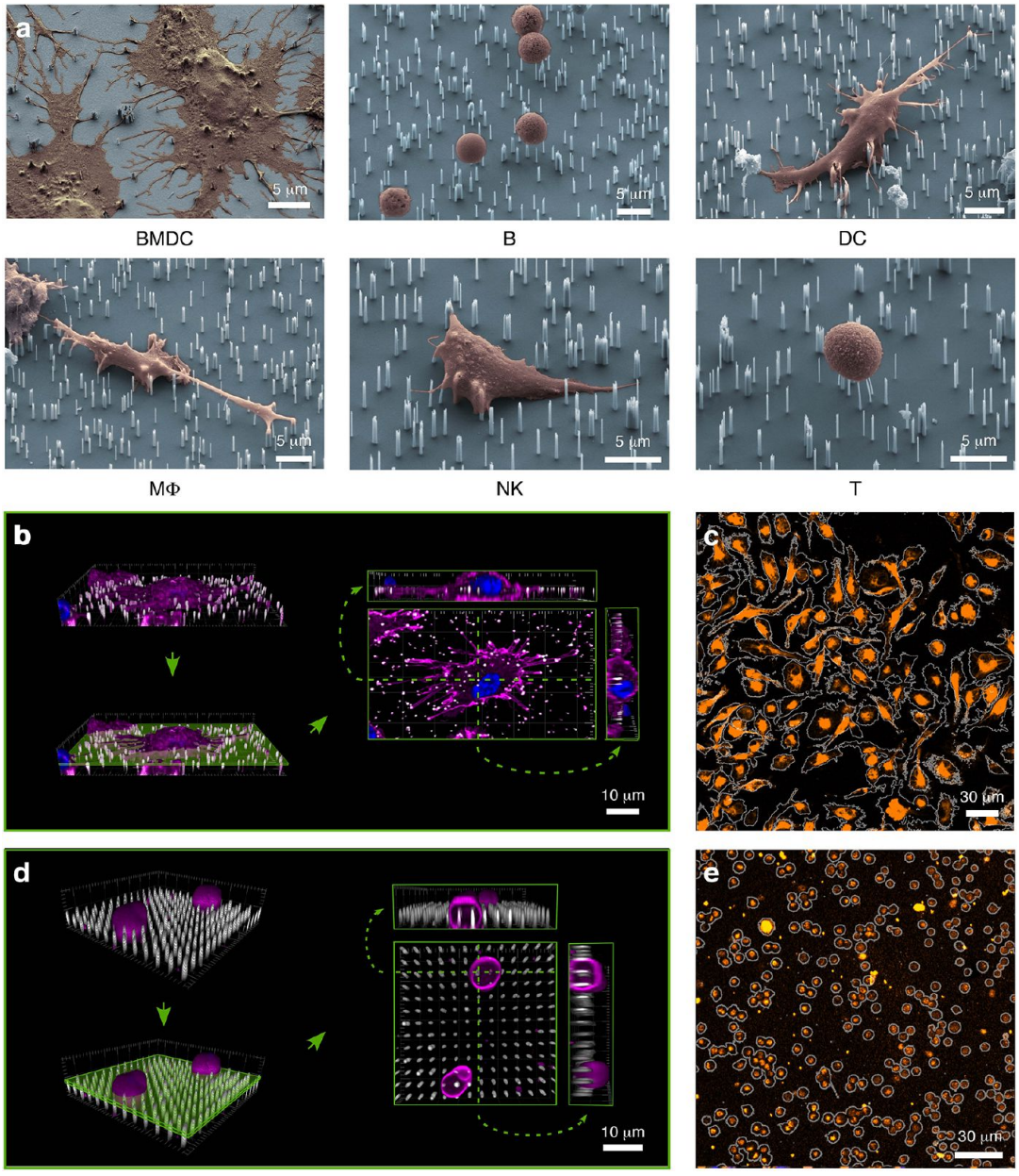

Figure 1. Nanowires (NWs) can deliver siRNA into ex vivo primary immune cells. (a) Scanning electron microscope images of mouse bone-marrow dendritic cells (BMDCs), B cells, dendritic cells (DCs), macrophages (MΦs), natural killer (NK) cells, and T cells (false colored orange) on top of NWs (false colored blue) taken 24 h after plating. (b) Three-dimensional reconstruction (left) of confocally imaged mouse BMDC (membrane: magenta, nucleus: blue) on top of Alexa-labeled NWs (white). Right center: confocal XY slice (green plane indicated on the left). Right top and far right: orthogonal XZ and YZ plane views (indicated by the dashed green lines). (c) Confocal microscope image showing Cy3-labeled siRNA (orange) delivered to mouse BMDCs (intact cytoplasms: gray outlines) using NWs. (d) Three-dimensional reconstruction (left) of confocally imaged human B cells (membrane: magenta) on top of Alexa-labeled NWs (white). (e) Confocal microscope image showing Cy3-labeled siRNA (orange) delivered to human B cells (intact cytoplasms: gray outlines) using NWs.

that NW-mediated delivery can be successfully applied in various cell lines and primary neurons and fibroblasts.[14] However, their utility in primary immune cells has yet to be investigated, and it was unknown if these cell types would sense NWs as foreign substances that could be activating or cause apoptosis. Additionally, different immune cells present vastly different morphologies, sizes, adhesive properties, and modes of function, and consequently, each provides distinct challenges for developing a universal delivery platform.

To develop a general NW-based delivery modality applicable for immune cells, we studied several mature immune cell subsets that were immunomagnetically (MACS) isolated from mouse bone marrow and spleen or from human blood samples. These cells included bone marrow derived dendritic cells (BMDCs, CD11c+), B cells (CD19+), dendritic cells (DCs, CD11c+), macrophages (MΦ, CD11b+), natural killer cells (NK, DX5+), and T cells (CD4+) (Figure S1). For each of the immune cell types, we optimized the physical parameters of our NWs (Figures 1 and 2, Figures S1−S13, Supporting Information (SI)). Effective delivery of biomolecules into smaller immune cells that grow in suspension (e.g., naïve mouse B and T cells) required the use of NWs that were longer

dx.doi.org/10.1021/nl3042917 | *Nano Lett.* 2012, 12, 6498−6504

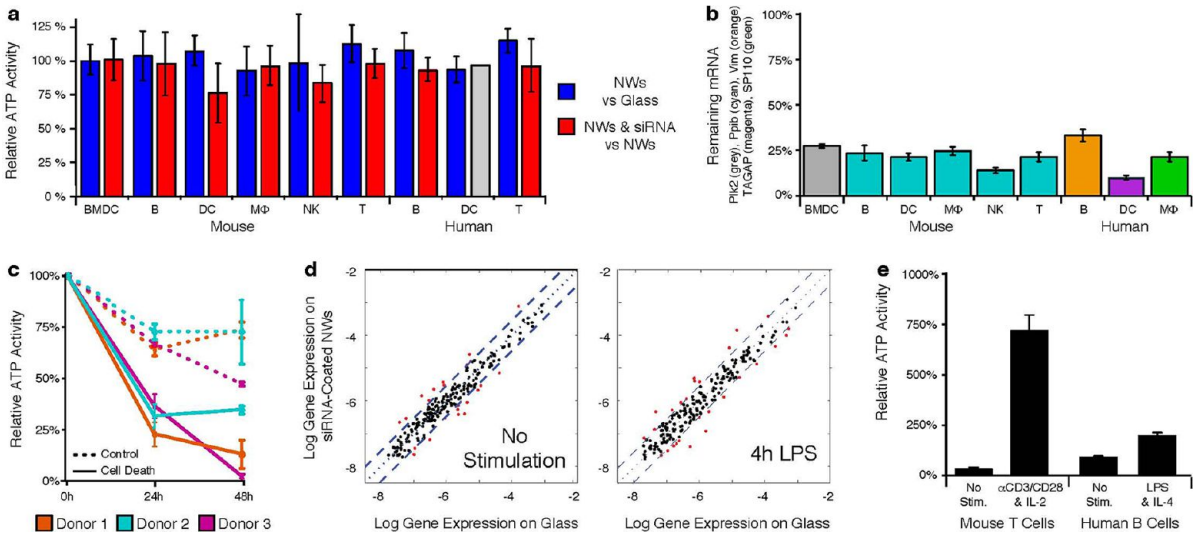

Figure 2. NW mediated delivery is minimally invasive, yet effective, in ex vivo primary immune cells. (a) Plating cells on NWs does not diminish cell viability relative to glass controls (blue); similarly, coating the NWs with siRNA has negligible impact on cell health (red) (n = 3). All values are mean ± standard error; light gray = not measured. (b) *Plk2* (gray), *Ppib* (cyan), *TAGAP* (magenta), and *SP110* (green) expression levels upon siRNA delivery. The degree of knockdown is measured by qRT-PCR, relative to *Gapdh/GAPDH*. Knockdowns: mouse BMDCs, 69 ± 1%; mouse B, 75 ± 4%; mouse DC, 77 ± 2%; mouse MΦ, 73 ± 2%; mouse NK, 85 ± 2%; mouse T, 77 ± 3%; human B,71 ± 4%; human DC, 90 ± 2%, and human MΦ, 78 ± 2%; all values are mean ± standard error for n = 10 (*Plk2*), n = 6 (*Ppib*), and n = 4 (*TAGAP, SP110*). (c) Cell viability measured (as ATP activity) on three different sets of human B cells receiving either non-targeting (NT) (dashed lines) or cell death inducing siRNA (CD) (solid lines) shows that administering CD siRNA effectively kills more cells than a non-targeting control. Values are mean ± standard error, n = 3. (d) SiNWs and their cargo neither active innate immune responses nor inhibit their induction with conventional stimuli. Similar gene expression levels (300-gene Nanostring immune response codeset) are observed in BMDCs whether they are plated on glass or NWs coated with siRNA, both in the presence and absence of lipopolysaccharide (LPS). Dashed lines represent 95% confidence intervals. (e) Mouse T and human B cells grow and divide on NWs when activated with conventional stimuli.

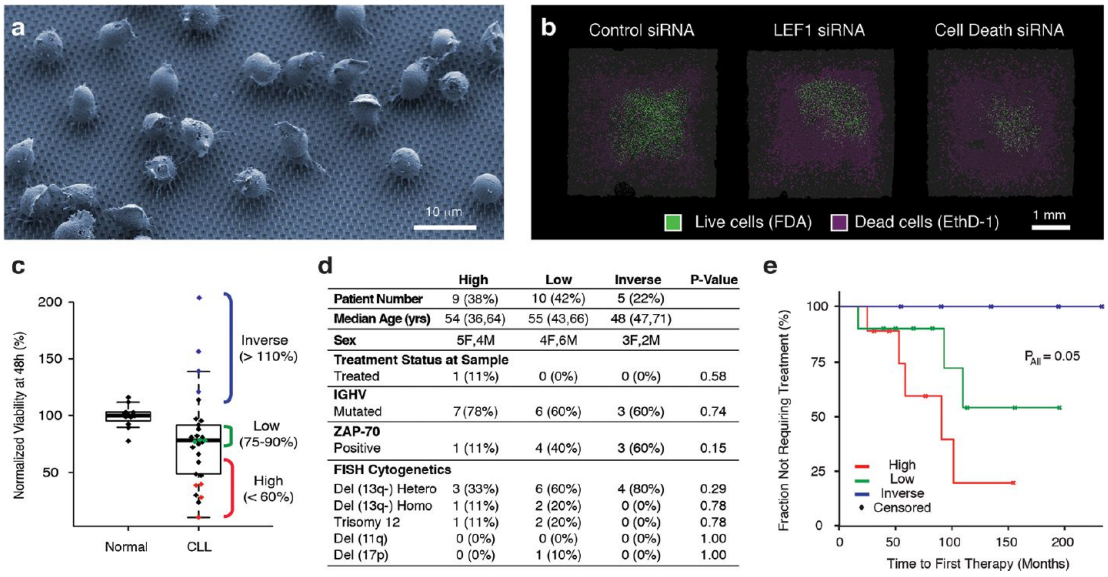

	High	Low	Inverse	P-Value
Patient Number	9 (38%)	10 (42%)	5 (22%)	
Median Age (yrs)	54 (36,64)	55 (43,66)	48 (47,71)	
Sex	5F,4M	4F,6M	3F,2M	
Treatment Status at Sample				
Treated	1 (11%)	0 (0%)	0 (0%)	0.58
IGHV				
Mutated	7 (78%)	6 (60%)	3 (60%)	0.74
ZAP-70				
Positive	1 (11%)	4 (40%)	3 (60%)	0.15
FISH Cytogenetics				
Del (13q-) Hetero	3 (33%)	6 (60%)	4 (80%)	0.29
Del (13q-) Homo	1 (11%)	2 (20%)	0 (0%)	0.78
Trisomy 12	1 (11%)	2 (20%)	0 (0%)	0.78
Del (11q)	0 (0%)	0 (0%)	0 (0%)	1.00
Del (17p)	0 (0%)	1 (10%)	0 (0%)	1.00

Figure 3. NWs successfully deliver *LEF1* siRNA into ex vivo human B cells obtained from normal donors and CLL patients, revealing functional heterogeneity that correlates with clinical outcome. (a) Scanning electron microscope images of CLL-B cells on top of NWs taken 24 h after plating. (b) CLL-B cells (intact cytoplasms: green, dead nuclei: magenta) on full 4 × 4 mm SiNW samples (dark gray squares) raster-imaged using a confocal microscope 24 h after plating. Administering a cell death inducing siRNA (far right) kills a larger number of cells than a non-targeting control (far left). The middle sample shows the effect of *LEF1* siRNA on CLL-B cell viability for one particular patient sample. (c) The effect of *LEF1* knockdown on the viability of normal B (n = 12) and CLL B-cells (n = 29), normalized to a non-targeting siRNA, shows tremendous heterogeneity across CLL patient samples (see SI Methods). Median viability for CLL samples is 78% versus 100% for normal donors (p_{CLL} = 0.005, p_{Normal} = 0.97, Wilcoxon signed rank test for comparison to nontargeting control siRNA; $p_{CLL\_vs\_Normal}$ = 0.004, Mann−Whitney rank sum test for comparison of CLL samples to normal samples). Patients are grouped into high, low and inverse responders based on their differential response. Colored points represent patient samples for which microarray profiles were generated. (d) Clinical characteristics of the 29 patients on whose CLL-B cells *LEF1* knockdowns were performed. (e) Kaplan−Meier curves of the high, low, and inverse responders.

dx.doi.org/10.1021/nl3042917 | *Nano Lett.* 2012, 12, 6498−6504

(2−3 μm), sharper (diameter <150 nm), and denser (0.3−1 per μm^2). These cells also needed increased preincubation periods to facilitate settling on top of the NWs. Larger, adherent immune cells (e.g., DC and MΦ) required the use of NWs that were slightly shorter (1−2 μm) and less dense (0.15−0.2 per μm^2). While longer NWs (>3 μm) proved minimally invasive to murine splenocytes and human B and T cells (Figure S2), they negatively impacted the viability of larger, adherent mouse and human immune cells (e.g., DC, MΦ, and BMDCs), likely due to nuclear disruption (Figure S3). As a general rule, we found that the NW density and, to a lesser extent, diameter needed to be scaled to match cell size and that the NW height required adjustment to facilitate cellular adhesion and penetration (see, for example, Figures 1d and S2).

Once the NW dimensions were optimized for each cell type, we observed that these NWs could consistently penetrate cellular membranes (Figures 1b and d, S2, and S3) without impacting cell health or morphology (Figures 1, 2a, 3a and b, and S2 through S13). When the NWs were precoated with fluorescently labeled siRNAs, plasmids, peptides, and proteins, these molecules were delivered into nearly every cell (Figures 1c, 1e, S7, and S8) without altering viability (Figures 2a, S4 through S6, see SI). Consistent with our previous findings in non-immune cells,[14] the biomolecular cargo delivered by the NWs was functional. In particular, siRNAs administered using NWs yielded substantial reductions (≥69%) in targeted mRNA levels and expected phenotypic changes in every immune cell type tested (Figures 2b and c, see SI).

Crucially, NW-mediated delivery neither activated an immune response nor interfered with normal immune sensing, cellular activation, or cell proliferation in response to physiological signals. First, when profiled with a signature set of 300 immune response genes (using the Nanostring nCounter technology,[11,15] Table S1), BMDCs plated on NWs coated with control siRNAs exhibited similar mRNA expression levels to BMDCs plated on glass, both prestimulation and in the presence of conventional stimuli, such as lipopolysachardide (LPS) (Figure 2d, see SI). Quantitative real-time polymerase chain reaction (qRT-PCR) for the major inflammatory cytokines[16] Tnf-α and Cxcl1, as well as virally induced[16] Cxcl10 and Type I Interferons (Ifns; e.g., Ifn-β), gave similar results both for control siRNAs and other biomolecules (see Figures S9 and S10). This result is likely due to the fact that NWs deliver cargo directly into the cytoplasm and hence bypass the endosomal pathway where innate immune sensing can occur.[1,9,11,16,17]

In fact, neither the NWs nor their biomolecular cargo spontaneously activated immune responses in any of the primary immune cells tested. Specifically, murine B cells, DCs, and MΦ plated on NWs all showed low basal expression levels of Tnf-α before stimulation and exhibited normal inflammatory responses to appropriate stimuli (see SI). Similar results were seen for NK and T cells based on Ifn-γ expression levels (Figure S11; see SI). Finally, mouse T cells and human B cells were able to expand on NWs in response to anti-CD3/anti-CD28 & IL-2 and LPS & IL-4 stimulation, respectively (Figures 2e, S12, and S13).

These findings demonstrate that NWs provide a potent, yet minimally invasive, means of delivering perturbants into a variety of murine and human immune cells ex vivo. NW-mediated delivery is effective for essentially all primary immune cell types without affecting viability (when compared to multiwell or glass coverslip controls; Figures 2a and S4 through S6), and neither activates nor prohibits conventional induction of innate immune responses (Figures 2d and S9 through S11).[1−3,6−10,12] The ability to deliver functional biomolecular cargo in a minimally invasive fashion provides a powerful new tool for studying the molecular circuitry governing the function of immune cells in both normal and diseased states.

To demonstrate this utility, we applied NW-based gene silencing to investigate the potential basis of clinical heterogeneity in chronic lymphocytic leukemia (CLL).[18,19] CLL, the most common adult leukemia in North America, is characterized by the progressive accumulation of dysfunctional mature B cells that have escaped normal apoptotic programs.[18,19] Despite the fact that CLL-B cells of different patients share a common immunophenotype, CLL patients exhibit tremendous variability in their response to treatment and in their overall survival.[18] While intensive research efforts over the past few decades have revealed much about this disease,[8,18−26] a clear understanding of the intracellular circuitry responsible for CLL has yet to emerge.[8,18,20]

Previous studies have shown that dysregulation of the Wnt signaling pathway, normally responsible for guiding proliferation and cell fate,[27−29] plays an important role in CLL.[19,22−24] By analyzing microarray data from 193 CLL-B samples, we indeed confirmed overall dysregulation of Wnt pathway components in CLL-B cells compared to normal CD19+ B cells[20] (see SI, Figure S14). We also found that *LEF1*, a terminal transcriptional activator of the Wnt signaling pathway previously linked to CLL-B cell survival,[22] was one of the most upregulated mRNAs in CLL compared to normal B cells.[30]

To test the importance of *LEF1* for CLL B-cell survival, we used NW-mediated siRNA delivery to silence its expression in B cells isolated from 29 CLL patients and 12 normal donors and examined cell survival 48 h after siRNA delivery (Figures 3a and b, S15 and S16, see SI). As a group, CLL-B cells exhibited lower viability (median 78%) upon *LEF1* knockdown than CD19+ B cells from normal donors (100%), in agreement with previous reports[20,22] (p = 0.004, Mann−Whitney rank sum test). This median response, however, did not fully capture the tremendous variation in the viability of different patients' CLL-B cells (ranging from 10 to 204%, Figure 3c). Notably, the observed response heterogeneity did not correlate with patients' *LEF1* expression levels (Figure S17), suggesting that the amount of *LEF1* mRNA is not sufficient to explain the observed heterogeneity. Silencing other core Wnt pathway members in CLL-B cells from the same set of patients yielded similar response heterogeneities (Figure S18), suggesting that Wnt signaling, rather than *LEF1* alone, influences CLL-B cell viability in a patient-specific fashion.

We separated the 29 tested patient CLL-B samples into three distinct groups based on the cells' survival in response to *LEF1* silencing: high responders (HRs, n = 9), whose CLL-B cell survival ratio (normalized to a nontargeting siRNA control) was less than 0.60; low responders (LRs, n = 10), displaying a survival ratio between 0.75 to 0.90; and, inverse responders (IRs, n = 5), with cell survival ratios in excess of 1.10. Five samples with intermediate phenotypes were excluded from our analysis to generate more clearly defined classes. These three patient groups were not enriched for any known CLL-associated prognostic features,[18,21] such as ZAP-70 expression or IgVH mutation status (Figure 3d, Fisher's exact test, p > 0.05), and could not be discerned using simple unbiased correlation metrics (either genome-wide or based on Wnt

dx.doi.org/10.1021/nl3042917 | Nano Lett. 2012, 12, 6498−6504

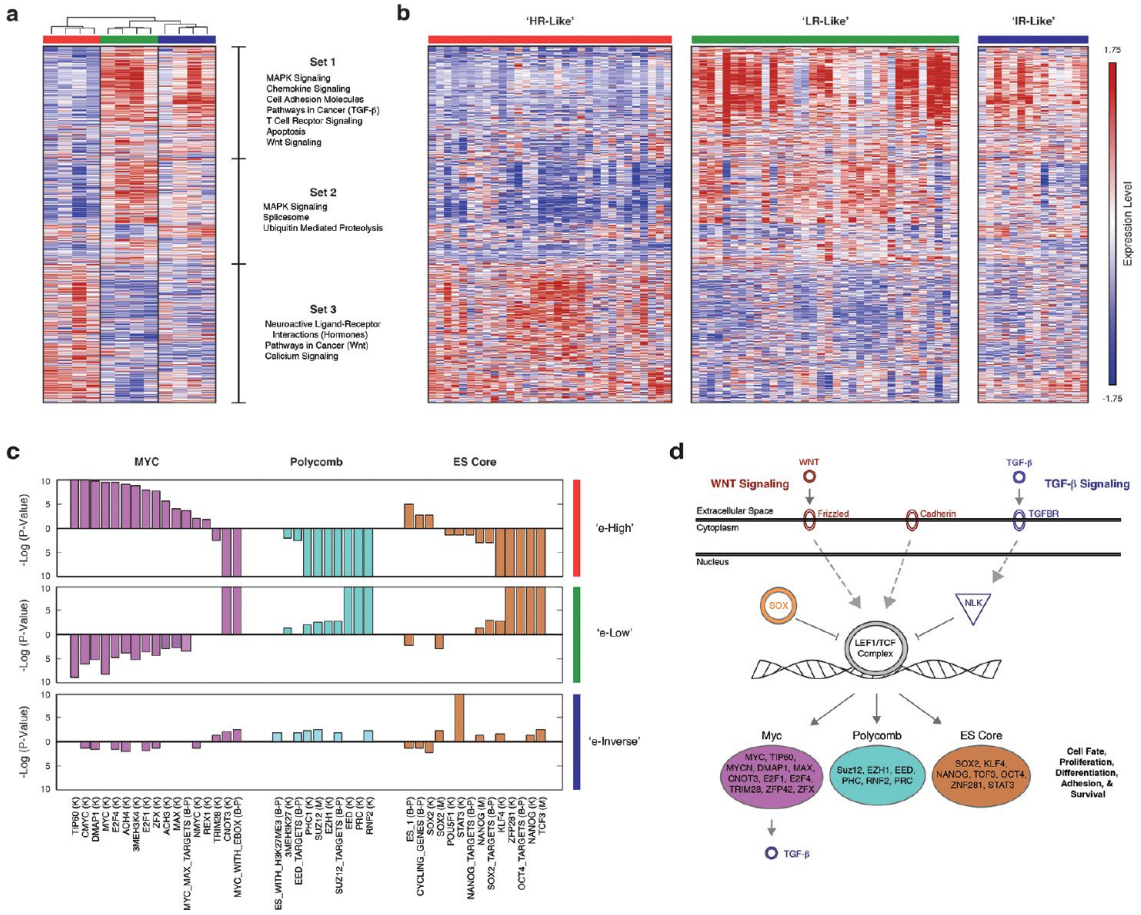

Figure 4. A potential mechanism for the effect of *LEF1* siRNA. (a) Expression heat map for the 823 genes that are significantly different between high- (HRs), low- (LRs), and inverse-responders (IRs), labeled as the red, green, and blue columns, respectively (n_{TOTAL} = 12 (4 per group); one-way ANOVA). (b) Of 181 additional patients for whom microarray data was available, 67 could be classified based on this ANOVA gene signature, yielding an additional 27 "HR-like", 30 "LR-like", and 10 "IR-like" responders (see SI Methods). These additional patients, when merged with the original 12 HRs, LRs, and IRs, form extended patient groups. The remaining 114 patients could not be clearly separated into one of the three categories (see SI Methods, Figures S18 and S20). (c) SS-GSEA of three gene modules—MYC, Polycomb, and ES Core—associated with HSCs and ESCs (see SI). Bar height represents the negative log of the enrichment while the direction of the bar indicates regulation. K, from reference 32; B–P, from ref 31; M, from ref 34 (see Table S2 for list members and *p*-values). (d) Model for observed effect of *LEF1* knockdown based on the SS-GSEA.

pathway member expression, Figure S19). Our patient groupings nevertheless exhibited statistically significant differences in their average time to first therapy (TTFT) (p = 0.05, Logrank test). For HRs, TTFT was 67.5 months (4 of 9 right censored), while the TTFTs for LRs and IRs were 85.5 months (7 of 10 right censored) and 123.2 months (all 5 patients right censored), respectively (Figure 3e). This analysis indicates that, strikingly, the response to even a single-gene silencing can be used to predict the clinical course of CLL patients.

To examine the molecular basis of this surprising finding, we compared the mRNA expression profiles from 12 of the 29 NW-tested samples (4 from each of the three classes for which microarray data was available) using a one-way analysis of variance (ANOVA). From this analysis, we identified 823 genes (out of 20 766 total) whose expression levels were significantly associated with the outcome of *LEF1* silencing (Figure 4a, Table S2, $p < 0.05$; see SI). Expression signatures for HRs and LRs were dramatically different from one another; IRs were more similar to LRs, but displayed depressed expression across many more genes. These differences were validated by qRT-PCR for selected marker genes (Figure S20).

When we examined the expression of the 823 genes in an additional 181 CLL-B samples for which genome-wide expression profiles were available, we found 27 additional patients with gene expression patterns that resembled HRs (designated "HR-like") and 30 and 10 additional patients showing patterns resembling LRs ("LR-like") and IRs ("IR-like"), respectively (Figures 4b and S21, see SI). When we performed a Kaplan–Meyer analysis on these extended patient groups (the original 12 patients from which the 823 gene set was identified, as well as the 67 additional HR-, LR-, and IR-like patients), we once again observed significant differences in TTFT (p = 0.001, Logrank test, Figures S22 and S23) and no enrichments for any known CLL-associated clinical prognostic markers[18,21] (Fisher's exact test, $p > 0.05$, Figure S22, see Table S2), confirming similarity between our extended groups and our original tested samples.

DAVID and single sample gene set enrichment analyses (SS-GSEA,[28,29] Figure 4a, see Tables S2 and S4 for full lists) showed that several canonical pathways commonly linked to CLL and other malignancies[20,25] were enriched among the 823 genes. In particular, many of the 823 genes were associated with stem-cell pathway regulation and hematopoietic lineage and

dx.doi.org/10.1021/nl3042917 | *Nano Lett.* 2012, 12, 6498–6504

development, consistent with the known roles of Wnt signaling (Tables S2 and S4). To explore this connection, we used SS-GSEA[28,29] to compare expression levels of gene sets[31−34] that characterize hematopoietic (HSC) and embryonic stem (ES) cells—an ES core, a Polycomb repressor complex (PRC), and a *MYC* module—across the patient groups (see SI). In HRs and the HR-like patient group, *MYC* and proliferation modules were elevated, whereas PRC and ES core modules were repressed, similar to what has been observed previously in short-term HSCs and many aggressive cancers[32] (Figure 4c, see Table S4). Conversely, LRs and the LR-like group showed a signature that resembles self-renewing long-term HSCs, including increased PRC and ES core components and repressed *MYC* and proliferation genes.[31,32] Finally, the IRs and the IR-like group presented a less distinctive signature, save for the induction of genes targeted by *STAT3*.

When integrated with information regarding the relative sensitivity toward *LEF1* knockdown, the results of the SS-GSEA analysis suggest specific hypotheses on the pathways contributing to differentiating the three patient classes. Namely, the expression patterns and *LEF1* sensitivity of HRs hint that Wnt signaling may influence CLL pathogenesis via regulation of *MYC* by the LEF1/TCF complex.[35] LRs and IRs, on the other hand, display enrichment for *MYC* targets with E-Box elements, such as TGF-β, suggesting interplay between the Wnt and TGF-β signaling pathways.[36,37] Elevated TGF-β signaling in LRs and IRs (Figure 4a) can, in part, explain the heterogeneity observed in response to *LEF1* knockdown because the TGF-β pathway can influence the LEF1/TCF complex via negative feedback[37−39] (Figure 4d).

Taken together, our results clearly show that NWs provide a minimally invasive method for effectively delivering biomolecules into primary immune cells, including naïve or resting cells, thereby enabling systematical analysis of cell circuits and functional responses in normal and malignant hematopoietic cells from both human and mouse. In particular, our studies demonstrate that the response to NW-mediated gene silencing can be related to clinical parameters in CLL and provide insight into the molecular circuitry contributing to disease heterogeneity. It is important to note that this NW-based perturbation strategy is fully extendable to other systems: starting from the cells taken from a single blood draw, NW-mediated gene silencing could be used to simultaneously probe the importance of each potential driver pathway in various hematological diseases, enabling not only the identification of gene signatures and pharmaceutical targets, but also the development of patient-specific combinatorial therapies.[30,40,41]

■ ASSOCIATED CONTENT

Supporting Information

Additional information on methods and any associated references. This material is available free of charge via the Internet at http://pubs.acs.org.

■ AUTHOR INFORMATION

Corresponding Author

*E-mail: Hongkun_Park@harvard.edu.

Author Contributions

These authors contributed equally to this work.

Notes

The authors declare no competing financial interest.

■ ACKNOWLEDGMENTS

H.P. was supported by an NIH Pioneer Award (5DP1OD003893-03), an NIH CEGS Award (1P50HG006193-01), and the Broad Institute. C.J.W. was supported by the Blavatnik Family Foundation, the Damon-Runyon Cancer Research Foundation (CI-38-07), an AACR SU2C Innovative Research Grant, HHMI Early Physician-Scientist Career Development Award, NHLBI (1RO1HL103532-01) and NCI (1R01CA155010-01A1). A.R. was supported by an NIH Pioneer Award, an NIH CEGS Award (1P50HG006193-01), HHMI, and the Merkin Foundation for Stem Cell Research at the Broad Institute. N.P. was supported by an FWO fellowship. N.H. was supported by an NIH grant (U54 AI057159) and an NIH New Innovator Award (DP2 OD002230). J.R.B. was supported by the American Society of Hematology and the Leukemia and Lymphoma Society. N.P. is a Broad Fellow of the Broad Institute and a postdoctoral research fellow of the Fund for Scientific Research—Flanders (FWO Vlaanderen), Belgium. H.P., C.J.W., A.R, and N.H. conceived the ideas and directed the work. A.S., C.W., and H.P. designed research. A.S., J.G., M.A., N.C., J.R., L.W., R.G., N.Y., and I.A. performed experiments. A.S., J.G., and H.P. wrote the manuscript; all authors read and edited the manuscript extensively.

■ REFERENCES

(1) Judge, A. D.; Sood, V.; Shaw, J. R.; Fang, D.; Mcclintock, K.; Maclachlan, I. *Nat. Biotechnol.* **2005**, *23* (4), 457−462.

(2) Shayakhmetov, D. M.; Paolo, N. C. D.; Mossman, K. L. *Mol. Ther.* **2009**, *18* (8), 1422−1429.

(3) Couto, L. B.; High, K. A. *Curr. Opin. Pharmacol.* **2010**, *10* (5), 534−542.

(4) Guignet, E. G.; Meyer, T. *Nat. Methods* **2008**, *5* (5), 393−395.

(5) Novina, C. D.; Murray, M. F.; Dykxhoorn, D. M.; Beresford, P. J.; Riess, J.; Lee, S.-K.; Collman, R. G.; Lieberman, J.; Shankar, P.; Sharp, P. A. *Nat. Med.* **2002**, 1−7.

(6) Dardalhon, V.; Herpers, B.; Noraz, N.; Pflumio, F.; Guetard, D.; Leveau, C.; Dubart-Kupperschmitt, A.; Charneau, P.; Taylor, N. *Gene Ther.* **2001**, *8* (3), 190−198.

(7) McManus, M.; Haines, B.; Dillon, C.; Whitehurst, C.; van Parijs, L.; Chen, J.; Sharp, P. *J. Immunol.* **2002**, *169* (10), 5754.

(8) Seiffert, M.; Stilgenbauer, S.; Döhner, H.; Lichter, P. *Leukemia* **2007**, *21* (9), 1977−1983.

(9) Kim, D. H.; Rossi, J. J. *Nat. Rev. Genet.* **2007**, *8* (3), 173−184.

(10) Filion, M.; Phillips, N. *Biochim. Biophys. Acta* **1997**, *1329* (2), 345−356.

(11) Takeuchi, O.; Akira, S. *Cell* **2010**, *140* (6), 805−820.

(12) Gresch, O.; Engel, F.; Nesic, D.; Tran, T.; England, H.; Hickman, E.; Körner, I.; Gan, L.; Chen, S.; Castro-Obregon, S. *Methods* **2004**, *33* (2), 151−163.

(13) Bowles, R.; Patil, S.; Pincas, H.; Sealfon, S. C. *J. Immunol. Methods* **2010**, *363* (1), 21−28.

(14) Shalek, A. K.; Robinson, J. T.; Karp, E. S.; Lee, J. S.; Ahn, D.-R.; Yoon, M.-H.; Sutton, A.; Jorgolli, M.; Gertner, R. S.; Gujral, T. S.; Macbeath, G.; Yang, E. G.; Park, H. *Proc. Natl. Acad. Sci. U.S.A.* **2010**, *107* (5), 1870−1875.

(15) Chevrier, N.; Mertins, P.; Artyomov, M. N.; Shalek, A. K.; Iannacone, M.; Ciaccio, M. F.; Gat-Viks, I.; Tonti, E.; DeGrace, M. M.; Clauser, K. R.; Garber, M.; Eisenhaure, T. M.; Yosef, N.; Robinson, J.; Sutton, A.; Andersen, M. S.; Root, D. E.; von Andrian, U.; Jones, R. B.; Park, H.; Carr, S. A.; Regev, A.; Amit, I.; Hacohen, N. *Cell* **2011**, *147* (4), 853−867.

(16) Amit, I.; Garber, M.; Chevrier, N.; Leite, A. P.; Donner, Y.; Eisenhaure, T.; Guttman, M.; Grenier, J. K.; Li, W.; Zuk, O.; Schubert, L. A.; Birditt, B.; Shay, T.; Goren, A.; Zhang, X.; Smith, Z.; Deering, R.; McDonald, R. C.; Cabili, M.; Bernstein, B. E.; Rinn, J. L.; Meissner,

A.; Root, D. E.; Hacohen, N.; Regev, A. *Science* **2009**, *326* (5950), 257−263.
(17) Heidel, J. D.; Hu, S.; Liu, X. F.; Triche, T. J.; Davis, M. E. *Nat. Biotechnol.* **2004**, *22* (12), 1579−1582.
(18) Zenz, T.; Mertens, D.; Küppers, R.; Döhner, H.; Stilgenbauer, S. *Nat. Rev. Cancer* **2010**, *10* (1), 37−50.
(19) Gandhirajan, R. K.; Staib, P. A.; Minke, K.; Gehrke, I.; Plickert, G.; Schlösser, A.; Schmitt, E. K.; Hallek, M.; Kreuzer, K.-A. *Neoplasia* **2010**, *12* (4), 326−335.
(20) Wang, L.; Lawrence, M. S.; Wan, Y.; Stojanov, P.; Sougnez, C.; Stevenson, K.; Werner, L.; Sivachenko, A.; DeLuca, D. S.; Zhang, L.; Zhang, W.; Vartanov, A. R.; Fernandes, S. M.; Goldstein, N. R.; Folco, E. G.; Cibulskis, K.; Tesar, B.; Sievers, Q. L.; Shefler, E.; Gabriel, S.; Hacohen, N.; Reed, R.; Meyerson, M.; Golub, T. R.; Lander, E. S.; Neuberg, D.; Brown, J. R.; Getz, G.; Wu, C. J. *N. Engl. J. Med.* **2011**, *365* (26), 2497−2506.
(21) Pleyer, L.; Egle, A.; Hartmann, T. N.; Greil, R. *Nat. Rev. Clin. Oncol.* **2009**, *6* (7), 405−418.
(22) Gutierrez, A.; Tschumper, R. C.; Wu, X.; Shanafelt, T. D.; Eckel-Passow, J.; Huddleston, P. M.; Slager, S. L.; Kay, N. E.; Jelinek, D. F. *Blood* **2010**, *116* (16), 2975−2983.
(23) Lu, D.; Liu, J. X.; Endo, T.; Zhou, H.; Yao, S.; Willert, K.; Schmidt-Wolf, I. G. H.; Kipps, T. J.; Carson, D. A. *PLoS ONE* **2009**, *4* (12), e8294.
(24) Wu, Q. L.; Zierold, C.; Ranheim, E. A. *Blood* **2009**, *113* (13), 3031−3039.
(25) Rodríguez, A.; Villuendas, R.; Yáñez, L.; Gómez, M. E.; Díaz, R.; Pollán, M.; Hernández, N.; de la Cueva, P.; Marín, M. C.; Swat, A.; Ruiz, E.; Cuadrado, M. A.; Conde, E.; Lombardía, L.; Cifuentes, F.; Gonzalez, M.; García-Marco, J. A.; Piris, M. A. *Leukemia* **2007**, *21* (9), 1984−1991.
(26) Dietrich, S.; Kramer, O. H.; Hahn, E.; Schafer, C.; Giese, T.; Hess, M.; Tretter, T.; Rieger, M.; Hullein, J.; Zenz, T.; Ho, A. D.; Dreger, P.; Luft, T. *Clin. Cancer Res.* **2012**, *18* (2), 417−431.
(27) Angers, S.; Moon, R. T. *Nat. Rev. Mol. Cell Biol.* **2009**, *10* (7), 468−477.
(28) Klaus, A.; Birchmeier, W. *Nat. Rev. Cancer* **2008**, *8* (5), 387−398.
(29) Mosimann, C.; Hausmann, G.; Basler, K. *Nat. Rev. Mol. Cell Biol.* **2009**, *10* (4), 276−286.
(30) Klein, U.; Tu, Y.; Stolovitzky, G. A.; Mattioli, M.; Cattoretti, G.; Husson, H.; Freedman, A.; Inghirami, G.; Cro, L.; Baldini, L.; Neri, A.; Califano, A.; Dalla-Favera, R. *J. Exp. Med.* **2001**, *194* (11), 1625−1638.
(31) Ben-Porath, I.; Thomson, M. W.; Carey, V. J.; Ge, R.; Bell, G. W.; Regev, A.; Weinberg, R. A. *Nat. Genet.* **2008**, *40* (5), 499−507.
(32) Kim, J.; Woo, A. J.; Chu, J.; Snow, J. W.; Fujiwara, Y.; Kim, C. G.; Cantor, A. B.; Orkin, S. H. *Cell* **2010**, *143* (2), 313−324.
(33) Novershtern, N.; Regev, A.; Friedman, N. *Bioinformatics* **2011**, *27* (13), i177−i185.
(34) Marson, A.; Levine, S. S.; Cole, M. F.; Frampton, G. M.; Brambrink, T.; Johnstone, S.; Guenther, M. G.; Johnston, W. K.; Wernig, M.; Newman, J.; Calabrese, J. M.; Dennis, L. M.; Volkert, T. L.; Gupta, S.; Love, J.; Hannett, N.; Sharp, P. A.; Bartel, D. P.; Jaenisch, R.; Young, R. A. *Cell* **2008**, *134* (3), 521−533.
(35) Yochum, G. S. *PLoS ONE* **2011**, *6* (4), e18966.
(36) Attisano, L.; Labbe, E. *Cancer Metast. Rev.* **2004**, *23* (1), 53−61.
(37) Roarty, K.; Baxley, S. E.; Crowley, M. R.; Frost, A. R.; Serra, R. *Breast Cancer Res.* **2009**, *11* (2), R19.
(38) Labbe, E.; Letamendia, A.; Attisano, L. *Proc. Natl. Acad. Sci. U.S.A.* **2000**, *97* (15), 8358.
(39) Yamada, M.; Ohnishi, J.; Ohkawara, B.; Iemura, S.; Satoh, K.; Hyodo-Miura, J.; Kawachi, K.; Natsume, T.; Shibuya, H. *J. Biol. Chem.* **2006**, *281* (30), 20749−20760.
(40) Irish, J. M.; Myklebust, J. H.; Alizadeh, A. A.; Houot, R.; Sharman, J. P.; Czerwinski, D. K.; Nolan, G. P.; Levy, R. *Proc. Natl. Acad. Sci. U.S.A.* **2010**, *107* (29), 12747−12754.
(41) Piening, B. D.; Wang, P.; Subramanian, A.; Paulovich, A. G. *Radiat. Res.* **2009**, *171* (2), 141−154.